PHYSICAL REVIEW B VOLUME 47, NUMBER 8 15 FEBRUARY 1993-II

Dispersive and nondispersive charge transport in a molecularly doped polymer with superimposed energetic and positional disorder

P. M. Borsenberger*
Office Imaging Division, Eastman Kodak Company, Rochester, New York 14650-1714

R. Richert and H. Bässler
Fachbereich Physikalische Chemie und Zentrum fur Materialwissenschaften der Philipps-Universität, D-3550 Marburg, Germany
(Received 13 July 1992; revised manuscript received 8 October 1992)

Time-of-flight photocurrent measurements of 1,1-bis(di-4-tolylaminophenyl)cyclohexane doped bisphenol-A-polycarbonate show dispersive features at low temperatures. Within the nondispersive regime, transients show anomalously broad tails of universal shape. Their relative width is in quantitative accord with Monte Carlo simulations of a material characterized by degrees of energetic and positional disorder that have previously been determined from the temperature and field dependencies of the mobility. The transition to dispersive transport, delineated by a change of the temperature dependence of the carrier mean transit time, occurs at a critical energetic disorder parameter as predicted by simulation. The effect of positional disorder is to decrease the slope of the trailing edge of the photocurrent transient.

I. INTRODUCTION

If an initially δ-shaped sheet of charge carriers moves across a sample under the influence of a field, it spreads by diffusion. As long as the field is small enough such that $eEa/2kT \ll 1$, a being a typical jump distance, and the medium is homogeneous, equivalent to the jump rate being a well-defined quantity in the case of incoherent transport, Einstein's law holds relating the diffusivity and mobility via $eD=\mu kT$. In this limit, the relative spatial width of the charge sheet evolves as

$$\langle \Delta x^2 \rangle^{1/2} / \langle x \rangle = \left[\frac{kT}{eE} \right] \left[\frac{2}{Dt} \right]^{1/2} \quad (1)$$

and the relative spread of the time-of-flight photocurrent transient becomes $\Delta t_T / t_T = (2kT/eEL)^{1/2}$. This is no longer true for disordered media in which transport is controlled by a distribution of transition rates reflecting the energetic or positional randomness of the medium. Under the action of a field, a packet of carriers spreads faster with time relative to the transit time because carriers that temporarily reside in unfavorable sites will be delayed and vice versa. As a consequence, the spatial variance of the packet yields an apparent diffusivity that exceeds the zero-field diffusivity and increases with field. This effect has been treated analytically by Rudenko and Arkhipov[1] for the case of multiple trapping in an exponential distribution of trapping states and by computer simulation for the hopping in a random medium in which disorder splits the transport level into a distribution of states (DOS) with a Gaussian envelope.[2,3] The effect is not limited to the motion of charged species as Bouchaud and Georges have demonstrated by considering hydrodynamic flow in porous media.[4]

The central limit theorem requires that for long times the mean velocity of a packet of carriers becomes time independent. The shape of the packet approaches a Gaussian although the spread remains anomalously large, formally accounted for by a deviation from Einstein's law. If the time to reach equilibrium exceeds the mean transit time $\langle t_T \rangle$ diffusion becomes anomalous, its signature being dispersive photocurrent transients.

The experimental manifestation of anomalous spreading of a carrier packet is the long tail of time-of-flight transients which otherwise exhibit well-developed plateaus indicative of quasi-Gaussian transport. They are often observed in disordered solids such as molecularly doped polymers[5-8] or main chain polymers such as poly(phenylenevinylene).[9] For materials in which intrinsic energetic disorder prevails, tail spreading could quantitatively be accounted for in terms of the disorder parameter $\hat{\sigma}=\sigma/kT$ measuring the width of the DOS, σ, relative to kT.[3]

The concept of disorder controlled hopping has recently been extended to explain the transition from nondispersive to dispersive transport, henceforth ND→D, usually observed in disordered solids upon lowering the temperature, i.e., increasing the effective disorder.[10,11] It was shown that knowledge of σ, derived from the temperature dependence of the mobility, is sufficient to predict the temporal features of the photocurrent measured under dispersive conditions in a quantitative manner. The material studied was *p*-diethylaminobenzaldehyde diphenylhydrazone for which the field and temperature dependencies of the mobility suggested that positional, off-diagonal disorder is negligible.[12]

In this work, the role of diagonal disorder on the ND→D transition is further explored. The material studied is 1,1-bis(di-4-tolylaminophenyl)cyclohexane (TAPC) doped bisphenol-A-polycarbonate (BPPC). Previous studies have suggested that off-diagonal disorder is significant in this material.[13] It will be shown that the disorder formalism provides a framework for describing

the ND→D transition in a quantitative manner. The variation of the slopes of the photocurrent transients in double-logarithmic representation is studied as a function of temperature in a systematic way to enable a critical comparison of transport in a random energy landscape versus the Scher-Montroll concept.[14] In the latter picture, pure positional disorder is cast into a waiting time distribution, $\psi(t) \propto t^{-(1+\alpha)}$, which translates into an algebraic photocurrent transient displaying two distinct slopes. We will demonstrate that a Scher-Montroll type of waiting time distribution is inappropriate for rationalizing charge transport in doped polymers.

II. EXPERIMENT

Figure 1 shows the molecular structures of TAPC and BPPC. The TAPC was synthesized by the method described by Rule, Berwick, and Contois,[15] which has been summarized previously.[16] The polycarbonate was obtained from General Electric as Lexan® 145. Films were prepared by dissolving a mixture of 75% TAPC and 25% BPPC in dichloromethane, then coating the resulting solution on Ni-coated polyethylene terephthalate substrates. To reduce the solvent concentration, the samples were heated to 40 °C for 24 h in air, then 100 °C for 1 h under vacuo. All coatings were prepared under ultraviolet-free yellow light at low relative humidities using dry reagent grade solvent. The samples were then coated with a 0.20-μm vapor deposited layer of α-Se followed by a 500-Å Au electrode. During the deposition of the α-Se and Au layers, the sample was attached to a liquid N_2 cooled block.

The mobilities were measured by conventional time-of-flight techniques which have been described elsewhere.[8,16] In brief, the displacement of a sheet of holes injected into the TAPC doped layer from an α-Se photoemitting electrode is time resolved. Photoexcitation of the α-Se was by 3-ns exposures of 440-nm radiation derived from a dye laser. To minimize distortion of the photocurrent transients, the magnitude of the injected charge was less than $0.05CV_0$, where C is the sum of the sample and stray capacitance and V_0 the applied voltage. The photocurrent transients were measured in air with a Tektronix model 2301 transient digitizer system.

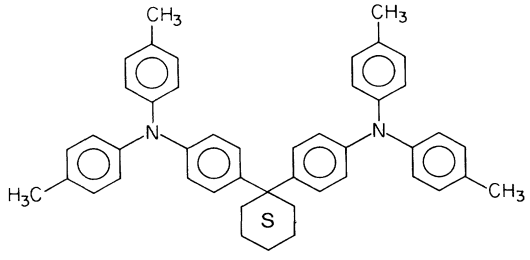

1,1-bis(di-4-tolylaminophenyl)-cyclohexane

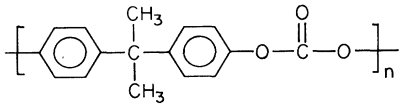

Bisphenol-A-polycarbonate

FIG. 1. The molecular structures of TAPC and BPPC.

III. RESULTS

Figures 2 and 3 illustrate a series of photocurrent transients in double-logarithmic and double-linear representation, respectively. The transients were measured at 3.6×10^5 V/cm, parametric in temperature. Photocurrent transients measured near room temperature display well-developed plateaus in double-linear representation, albeit with anomalously broad tails. At lower temperatures, the transients become progressively dispersive. Reducing the field to 9×10^4 V/cm leaves the general pattern unchanged. Plotting mobilities derived from mean carrier arrival times $\langle t_T \rangle$ inferred from the intersection of asymptotes in double-logarithmic representation as a function of T^{-2} yields two intersecting straight lines, as shown in Fig. 4. The slope T_0 of the high-temperature portion of the data at 9×10^4 V/cm is 729 K.

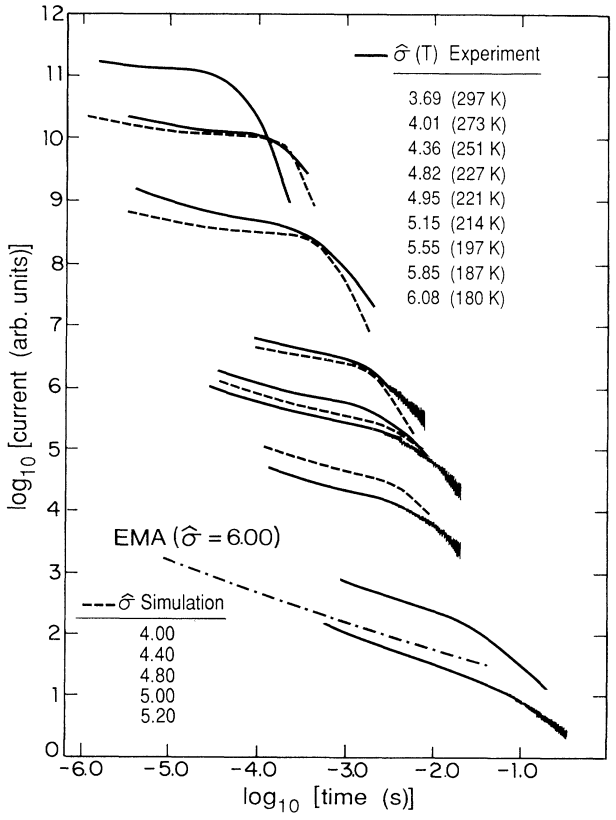

FIG. 2. Photocurrent transients, parametric in $\hat{\sigma}$ and temperature, in double-logarithmic representation. The thickness was 6.75 μm. The dashed curves are the results of computer simulations from Ref. 11 and assume $\sigma=0.095$ eV. The dashed curve for $\hat{\sigma}=6.0$ is the result of an analytic effective medium treatment from Ref. 19.

Although double-logarithmic plots deviate systematically from the algebraic behavior predicted by the Scher-Montroll formalism, one can nevertheless attempt to determine dispersion parameters from the asymptotes near the point of intersection, equivalent to approximating the temporal features of the photocurrent as

$$i(t) \propto \begin{cases} t^{-(1-\alpha_1)}, & t < \langle t_T \rangle \\ t^{-(1+\alpha_2)}, & t > \langle t_T \rangle \ . \end{cases} \tag{2}$$

Figure 5 shows that the parameter $1+\alpha_2$ increases with increasing temperature while $1-\alpha_1$ decreases with increasing temperature. Further, α_1 and α_2 are in general different with $\alpha_2 > \alpha_1$ for $T > 260$ K and vice versa. Within the limit of experimental resolution, no field dependence of α_1 or α_2 can be distinguished.

IV. DISCUSSION

The central purpose of this work is to determine whether the disorder model can explain the variation of

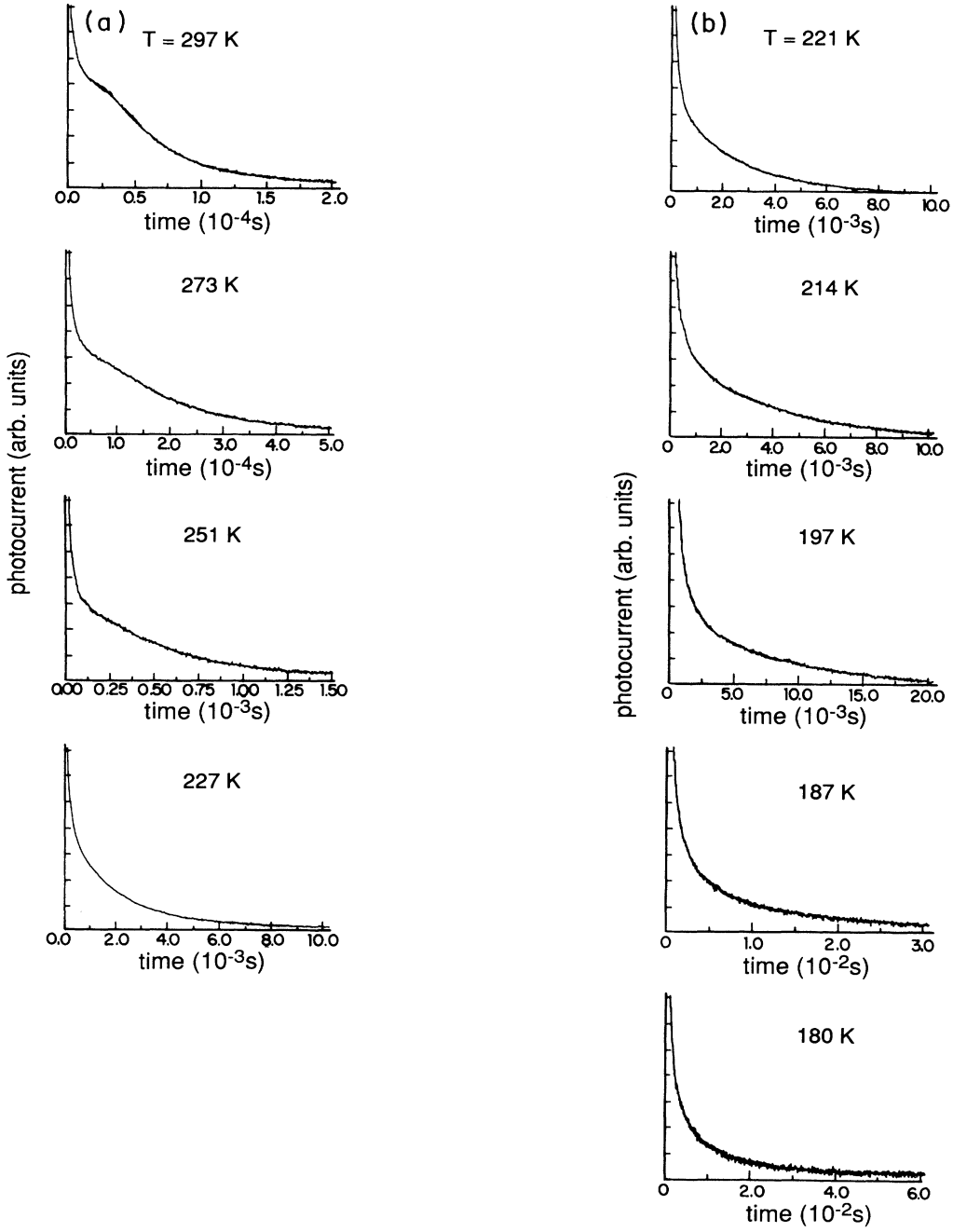

FIG. 3. Photocurrent transients, parametric in temperature, in double-linear representation. The thickness was 6.75 μm.

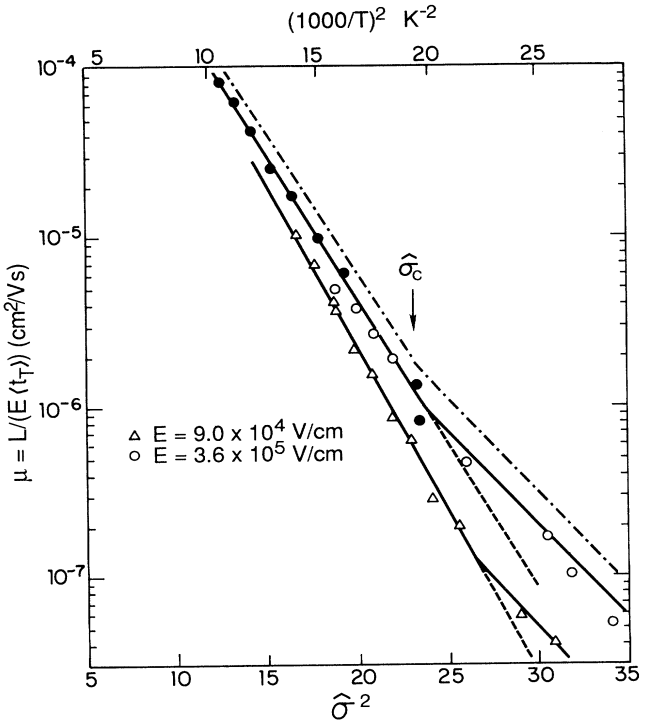

FIG. 4. $\log_{10}(L/E\langle t_T\rangle)$ vs T^{-2} and $\hat{\sigma}^2$. The solid circles are data taken from Ref. 13. The dashed curve is the prediction of simulations for $L=6.75$ μm, $\sigma=0.095$ eV, and $E=6\times10^5$ V/cm. The critical disorder parameter above which $\langle t_T\rangle$ no longer yields thickness-independent mobilities is indicated as $\hat{\sigma}_c$.

photocurrent transients with temperature and field in a material with superimposed energetic (diagonal) and positional (off-diagonal) disorder. This requires knowledge of the disorder parameters σ and Σ, being the Gaussian widths related to the random variables energy and overlap parameter, respectively. The former can be derived from the temperature dependence of the mobility at a field of the order of 10^5 V/cm at which the mobility either becomes independent of field or, in the case of large Σ, reaches a minimum,[13]

$$\mu(\hat{\sigma},E\simeq10^5\ \text{V/cm})=\mu_0\exp\left[-\left[\frac{2\hat{\sigma}}{3}\right]^2\right]. \quad (3)$$

Off-diagonal disorder, characterized by the variance Σ of the wave-function overlap parameter $2\gamma a$ in a Miller-Abrahams type expression for the transition rate,[13] can be determined from the slope of the linear portion of plots of the logarithm of the mobility versus $E^{1/2}$ where the slope is given as $\beta=C(\hat{\sigma}-\Sigma^2)$. Here C is an empirical constant given as 2.9×10^{-4} (cm/V)$^{1/2}$. The width of the DOS, σ, is related to T_0 as $\sigma=3kT_0/2$, thus $T_0=729$ K corresponds to $\sigma=0.095$ eV. In a previous study of 75% TAPC doped BPPC, σ and Σ were determined as 0.095 eV and 3.1, respectively.[13]

The time dependence of the mean-square displacement of an ensemble of carriers randomly injected from a photoemitting electrode such as α-Se into a manifold of hopping states is caused by energetic relaxation.[10] If equilibrium is attained before the carriers transit the thickness L, the transport acquires Gaussian features, albeit with anomalously large diffusivity to mobility ratios. In that case, the photocurrent transient is expected to follow[3]

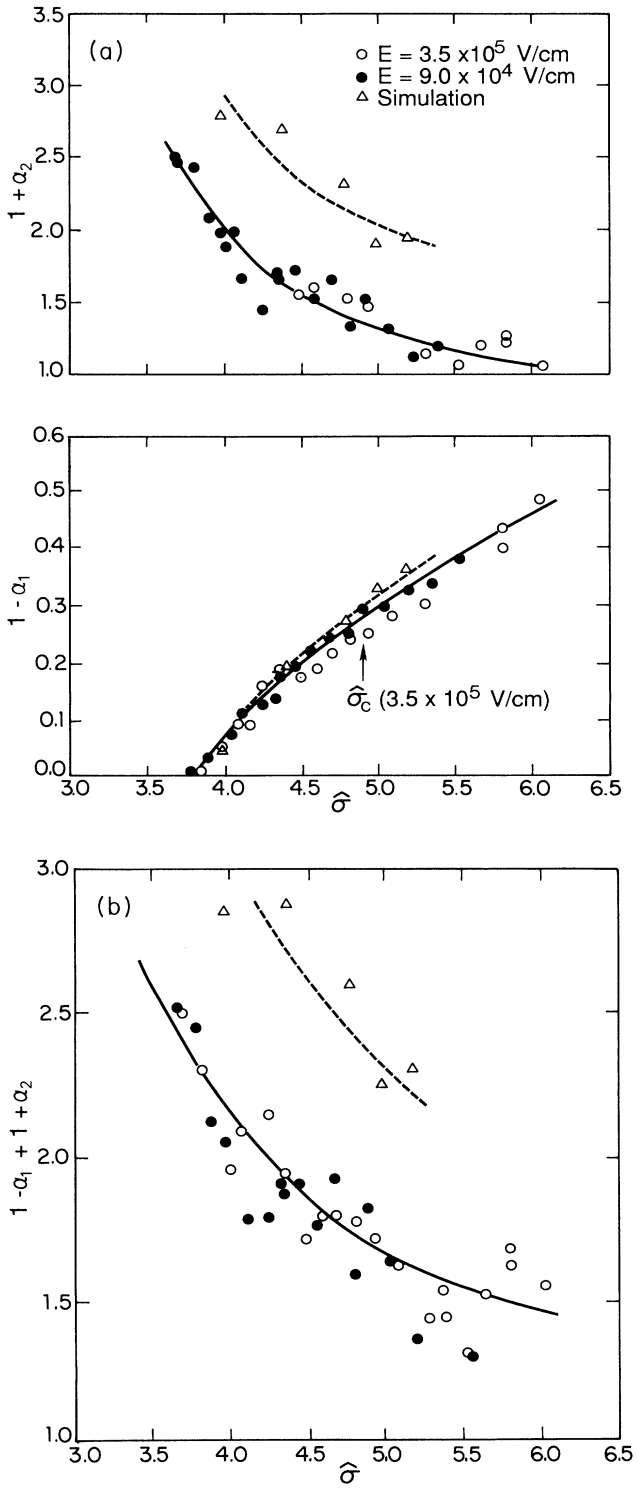

FIG. 5. Slope values $1-\alpha_1$ and $1+\alpha_2$ (a) and $1-\alpha_1+1+\alpha_2$ (b) vs $\hat{\sigma}$. The thickness was 6.75 μm.

$$i(t)=\int_0^L (4\pi Dt)^{-1/2}\exp\left[-\frac{(x-\mu Et)^2}{4Dt}\right]dx$$
$$=1-\tfrac{1}{2}\,\mathrm{erfc}\left[\frac{(L-\mu Et)}{2\sqrt{Dt}}\right]. \quad (4)$$

Experimental transients displaying at least a short plateau can be fitted to Eq. (4) over typically one order of magnitude in amplitude yielding $f=eD/\mu kT$ as a function of $\hat{\sigma}$ and E. This is illustrated in Fig. 6. Note, however, that Eq. (4) does not predict a power-law dependence of the photocurrent in double-logarithmic representation since

$$\frac{d\ln i}{d\ln t}=\frac{-\pi^{-1/2}\exp\left[-\left[\frac{L-\mu Et}{2\sqrt{Dt}}\right]^2\right]\left[\frac{\mu Et+L}{4\sqrt{Dt}}\right]}{1-\tfrac{1}{2}\,\mathrm{erfc}\left[\frac{L-\mu Et}{2\sqrt{Dt}}\right]} \quad (5)$$

is not a constant in the $t\to\infty$ limit. The fact that transients that exhibit a short plateau region, considered to be a signature of nondispersive transport, and feature a tail decaying as $t^{-(1+\alpha_2)}$ is, therefore, an indication that the asymptotic limit has not been strictly attained in samples typically 10 μm in length and characterized by a disorder parameter $\hat{\sigma}=3.5\ldots4.0$. Simulations recovering the temporal evolution of the spatial variance of a carrier packet, $\langle(x-\langle x\rangle)^2\rangle$, in samples with the above disorder parameters confirm this. In passing, we note that Eq. (4) predicts

$$\left.\frac{d\ln i}{d\ln t}\right|_{t=t_{1/2}}=(\mu V/\pi D)^{1/2}, \quad (6)$$

which is identical with the reciprocal variance $d^{-1}=t_{1/2}/(t_{1/2}-t_0)$ of the tails of photocurrent transients in double-linear representation. Here, $t_{1/2}$ is the time at which the current decays to one-half of the plateau value and t_0 marks the intersection of the asymptotes. The mean arrival times described in the simulations closely correspond to $t_{1/2}$.[3] Equation (6) provides a simple way of estimating the $eD/\mu kT$ ratio from transients in double logarithmic representation.

Values of $eD/\mu kT$ obtained for $T=297$, 271, and 260 K, equivalent to $\hat{\sigma}=3.69$, 4.04, and 4.21, respectively, are illustrated in Fig. 7 together with the results of previous simulations[3,17] for the parameter sets $\hat{\sigma}=1.5$, $\Sigma=3.25$ and $\hat{\sigma}=2.5$, $\Sigma=3.25$. Unfortunately, the increase in computational time with increasing $\hat{\sigma}$ prevents simulations at larger values of $\hat{\sigma}$ with superimposed off-diagonal disorder. It is, nevertheless, obvious that the field dependence of experimental $eD/\mu kT$ values is in accord with simulations, bearing out a $eD/\mu kT\propto E^{1.2}$ relationship which, in reality, will be difficult to distinguish from a linear relationship.

For pure energetic disorder, $eD/\mu kT\propto E^2$ has been found over a fairly wide range of fields with a tendency to saturate and decrease at high fields. Considering that the spread of the leading edge of the transients is proportional to $D/\mu EL$, this proves that the universality often seen in nondispersive transients parametric in field[6,18] is a consequence of the distribution of transition rates implied by the simultaneous presence of diagonal and off-diagonal

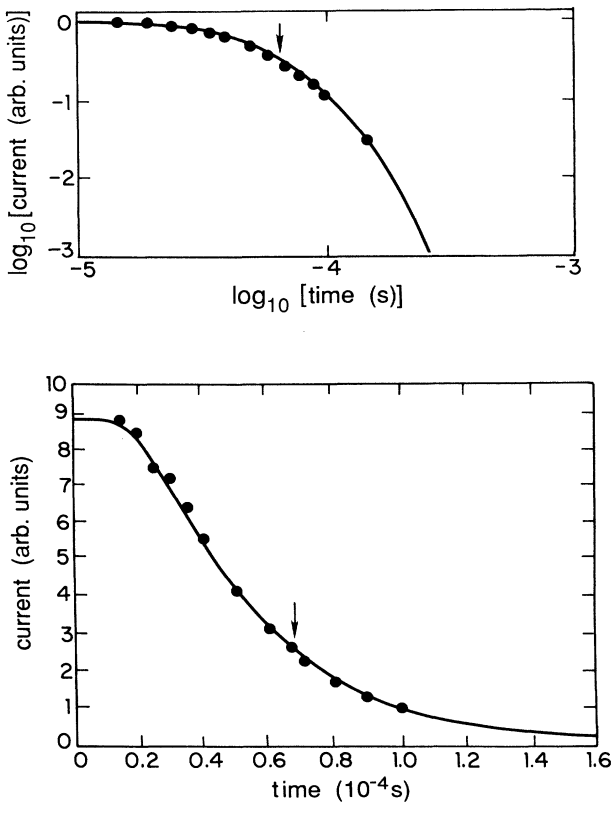

FIG. 6. Analysis of a photocurrent transient by Eq. (4) in double-logarithmic (a) and double-linear (b) representation. The arrows mark the mean carrier arrival time. The temperature was 298 K, the field 3.6×10^5 V/cm, and the thickness 6.75 μm.

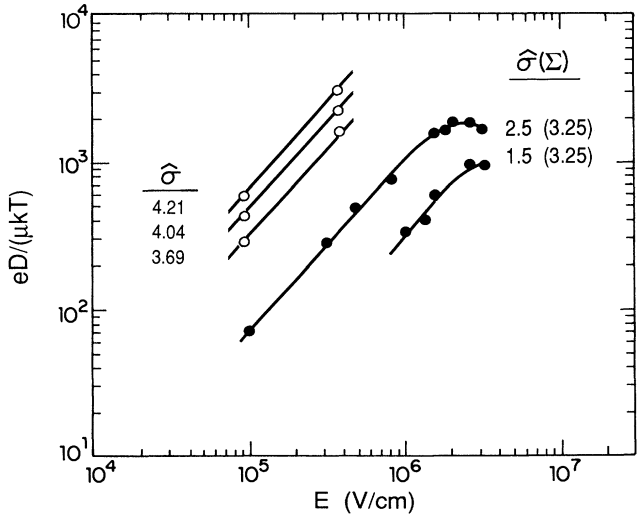

FIG. 7. Experimental (open circles) and simulated (solid circles) values of $eD/\mu kT$ vs E. The thickness was 6.75 μm. The simulations are from Refs. 3 and 17.

disorder. Quantitative consistency between simulation and experiment, as the dependence of $eD/\mu kT$ on $\hat{\sigma}$ is concerned, is indicted in Fig. 8. The data fall on the extrapolation of the simulation results. They exceed the values expected if off-diagonal disorder were negligible by a factor of 5, demonstrating that the information regarding disorder extracted from either the field and temperature dependencies of the mobility, or the temporal features of the photocurrent transients, is mutually consistent.

The ND→D transition shall be analyzed next. Although the energetic relaxation of an ensemble of excitations migrating via exchange interaction, such as triplet excitations,[19] has been studied experimentally and found to be consistent with the predictions of both analytic work[20] and simulations, its temporal course cannot be cast into a simple analytic relationship. This is an unfortunate consequence of the Gaussian-shaped DOS, borne out by inhomogeneously broadened absorption profiles of random organic solids. One has, therefore, to rely on the comparison between simulations or numerical solutions of analytic theory, and experiment.

Figure 2 shows photocurrent transients simulated[11] for samples of 8000 lattice planes, equivalent to a length of 4.8 μm, parametric in $\hat{\sigma}$, and vanishing off-diagonal disorder. The plot for $\hat{\sigma}=5.2$ is an extrapolation of data obtained with a 2.4 μm sample. It is obvious that the current decay prior to the inflection in double-logarithmic representation is well reproduced by simulation, yet the transition near $\langle t_T \rangle$ occurs more smoothly

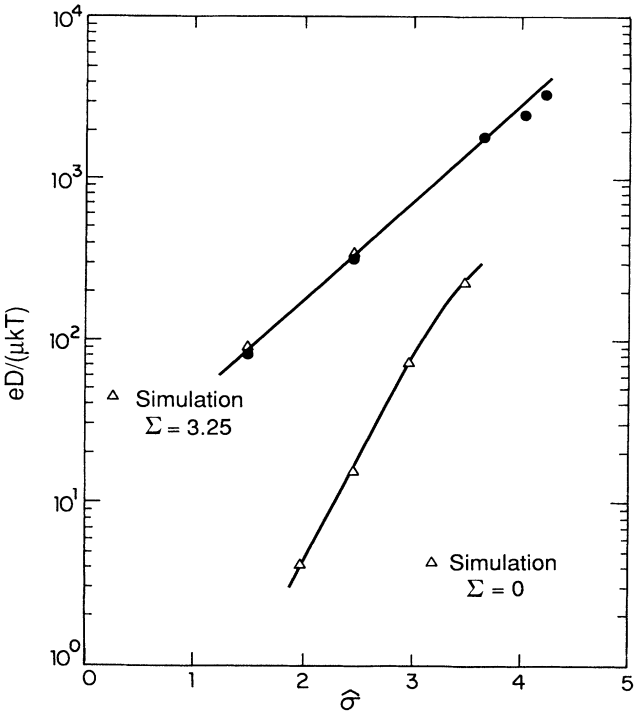

FIG. 8. Experimental (solid circles) and simulated (open triangles) values of $eD/\mu kT$ vs $\hat{\sigma}$. The field was 3.6×10^5 V/cm and the thickness was 6.75 μm.

and the slope for $t > \langle t_T \rangle$ is less than predicted. These results are summarized in Fig. 5, comparing experimental and simulation results for $1-\alpha_1$ and $1+\alpha_2$. Interpretation of this result is straightforward. For $t \ll \langle t_T \rangle$, the relaxation of the photocurrent is essentially determined by the energetic relaxation of the carriers within the DOS and the concomitant reduction of their mean velocity, spatial broadening of the carrier packet being unimportant. To first order, the presence of off-diagonal disorder does not alter the relaxation pattern except for a shift of the time frame towards shorter times. This agrees with earlier simulations of Marshall.[21] It does, however, increase the apparent field-dependent diffusivity that causes the carrier packet to spread faster, equivalent to a larger spread of momentary carrier velocities. The signature of this effect is the flattening of the transition region in the transient and the slower decay of the photocurrent at $t > \langle t_T \rangle$. Note that $1+\alpha_2$ decreases by typically 0.8 upon increasing Σ from zero to values of order 3.

The absence of a significant influence of the field on the slope parameters can be accounted for by the mutual cancellation of two opposing effects. On the one hand, an increasing field shortens the time available for carriers to relax energetically. Therefore, the degree of dispersion seen in photocurrent transients at $t \lesssim \langle t_T \rangle$ is expected to increase with increasing field. On the other hand, a field increases the mean equilibrium energy of carriers within the DOS with the consequence that the relaxation time is shortened.

A complementary way of analyzing the ND→D transition is by considering the temperature dependence of $L/(E\langle t_T \rangle)$. In the case of nondispersive transport, this is equal to the mobility. It has been shown in previous work[11] that the ND→D transition is manifested by a break in the $\langle t_T \rangle$ versus $\hat{\sigma}^2$ plot at a critical disorder parameter that depends on sample thickness according to the empirical relationship $\hat{\sigma}_c^2 = 44.8 + 6.7 \log_{10}(L)$, where L is the thickness in cm. Figure 4 compares experimental data with the prediction for a sample of $L=6.75$ μm, $E=6\times10^5$ V/cm, and experimental values of the low-field mobility. The result obtained for $E=3.6\times10^5$ V/cm is very close to the simulation result. Reducing the field shifts $\hat{\sigma}_c$ to somewhat larger values without, however, changing the overall pattern. Bearing in mind that the simulations were done on samples in the absence of off-diagonal disorder, this agreement is another way of demonstrating that off diagonal is unimportant as far as the temperature dependence of the mean carrier arrival time is concerned. It only affects the absolute time scales, pulse shapes, and the field dependence of the mobility.

The kink in $\langle t_T \rangle$ versus $\hat{\sigma}^2$ or T^{-2} plots that marks the ND→D transition correspond to transients that no longer exhibit a plateau but are characterized by $\alpha_2 = 0.7 \ldots 0.75$, indicating that the distinction between dispersive and nondispersive transients becomes a matter of definition, if not semantics. What we wish to point out here is that transients measured at temperatures such that $\hat{\sigma} < \hat{\sigma}_c$ yield mobilities that represent bulk properties, while transients measured at $\hat{\sigma} > \hat{\sigma}_c$ depend on the sample dimension.

It is tempting to compare the present results concern-

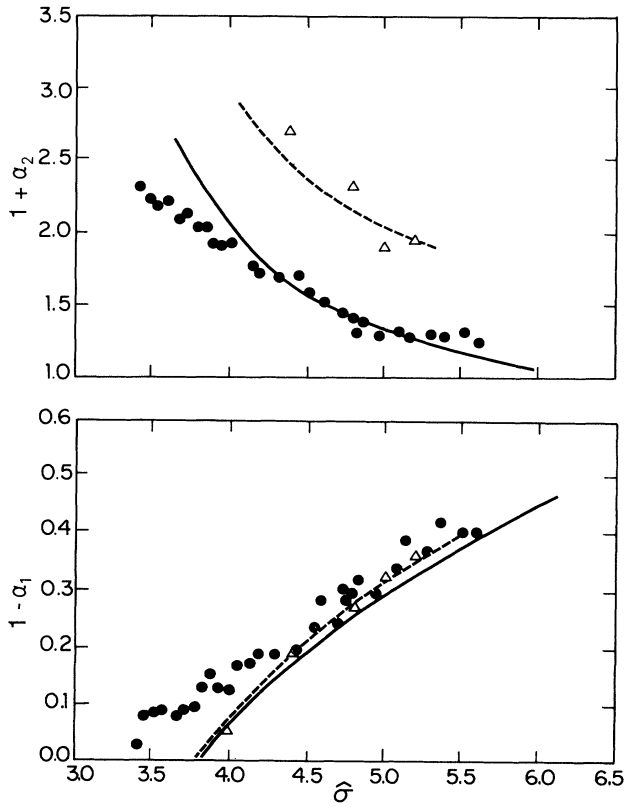

FIG. 9. Comparison of $1-\alpha_1$ and $1+\alpha_2$ for poly(*N*-vinylcarbazole) (PVK) (solid circles), TAPC doped BPPC (solid line), and simulations (dashed line and open triangles). The data for PVK have been calculated for $\sigma=0.110$ eV. The simulations were based on the assumption $\Sigma=0$.

ing the slope parameters $1-\alpha_1$ and $1+\alpha_2$ with literature results on poly(*N*-vinylcarbazole). Translating the activation energy of the mobility of Pfister and Griffith[22] into a width of the DOS yields $\sigma=0.110$ eV. This allows plotting $1-\alpha_1$ and $1+\alpha_2$ versus $\hat{\sigma}$. The results are illustrated in Fig. 9. The similarity with the present data is obvious. Remarkably, both $1-\alpha_1$ and $1+\alpha_2$ as a function of $\hat{\sigma}$ approach the TAPC doped BPPC data for $\hat{\sigma}>4.4$. Apart from the ambiguity involved in determining $1-\alpha_1$, the most plausible explanation for the deviations occurring at $\hat{\sigma}<4.4$ is related to trapping by carbazole sandwich pairs. This gives rise to additional dispersion, particularly at higher temperatures at which dispersion due to intrinsic disorder becomes small. A cautionary remark is, however, in order concerning the interpretation of any deviation between experimental $1+\alpha_2$ data and simulation results. Any type of disorder superimposed onto intrinsic energetic disorder will enhance spreading of the carrier packet and, concomitantly, reduce the value of $1+\alpha_2$. The effect of multiple trapping[23] due to a distribution of trapping states outside the intrinsic DOS cannot, therefore, be distinguished from that of off-diagonal disorder on the basis of photocurrent transients alone.

V. CONCLUDING REMARKS

This work confirms that the systematic temperature-dependent variations of the slopes of photocurrent transients of disordered molecular solids in double-logarithmic representation can be predicted in a quantitative manner on the basis of the disorder model employing parameters derived from the field and temperature dependencies of the mobility in the nondispersive regime. This conclusion is valid for materials with and without positional disorder superimposed onto intrinsic energetic disorder of the hopping site manifold. It also demonstrates that the previously noted failure to analyze dispersive photocurrent transients in terms of the Scher-Montroll theory, predicting that the sum of the slopes adds to 2, is a signature of the stochastic character of hopping with a Gaussian DOS that determines the distribution of elementary jump rates.

ACKNOWLEDGMENTS

The authors are grateful to J. Henry and E. Magin for experimental assistance and L. Pautmeier for unpublished simulation data. The financial support by the Deutsche Forschungsgemeinshaft and the Fonds der Chemischen Industrie is also gratefully acknowledged.

*Author to whom correspondence should be addressed.

[1]A. I. Rudenko and V. I. Arkhipov, Philos. Mag. B **45**, 177 (1982).
[2]R. Richert, L. Pautmeier, and H. Bässler, Phys. Rev. Lett. **63**, 547 (1989).
[3]L. Pautmeier, R . Richert, and H. Bässler, Philos, Mag. B **63**, 587 (1991).
[4]J. P. Bouchaud and A. Georges, C.R. Acad. Sci. Ser. B **307**, 1431 (1989); Phys. Rev. Lett. **63**, 2692 (1989).
[5]L. B. Schein, A. Rosenberg, and S. L. Rice, J. Appl. Phys. **60**, 4287 (1986).
[6]H. J. Yuh and M. Stolka, Philos. Mag. B **58**, 539 (1988).
[7]A. Peld and L. B. Schein, Chem. Phys. Lett. **153**, 422 (1988).
[8]P. M. Borsenberger, J. Appl. Phys. **68**, 6263 (1990).
[9]M. Gailberger and H. Bässler, Phys. Rev. B **44**, 8643 (1991).
[10]L. Pautmeier, R. Richert, and H. Bässler, Philos. Mag. Lett. **59**, 325 (1989).
[11]P. M. Borsenberger, L. Pautmeier, and H. Bässler, Phys. Rev. B **46**, 12 145 (1992).
[12]P. M. Borsenberger, Adv. Mater. Opt. Electron. **1**, 73 (1992).
[13]P. M. Borsenberger, L. Pautmeier, and H. Bässler, J. Chem. Phys. **94**, 5447 (1991).
[14]H. Scher and E. W. Montroll, Phys. Rev. B **12**, 2455 (1975).
[15]N. G. Rule, M. A. Berwick, and L. E. Contois, U.S. Patent No. 4,127,412 (28 November 1978).
[16]P. M. Borsenberger, J. Appl. Phys. **68**, 5682 (1990).
[17]L. Pautmeier (unpublished).
[18]M. Abkowitz, H. Bässler, and M. Stolka, Philos. Mag. B **63**, 201 (1991).
[19]R. Richert, H. Bässler, B. Ries, B. Movaghar, and M. Grünewald, Philos. Mag. Lett. **59**, 95 (1989).
[20]B. Movaghar, M. Grünewald, B. Ries, H. Bässler, and D. Würtz, Phys. Rev. B **33**, 5545 (1986).
[21]J. M. Marshall, Philos. Mag. B **47**, 323 (1983).
[22]G. Pfister and C. H. Griffith, Phys. Rev. Lett. **40**, 659 (1978).
[23]E. Müller-Horsche, D. Haarer, and H. Scher, Phys. Rev. B **35**, 1273 (1987).